American Journal of Engineering and Applied Sciences

Original Research Paper

The Study of the Dynamics of a Basic DoF Robot

Relly Victoria Virgil Petrescu

Department of Transportation, Traffic and Logistics, Bucharest Polytechnic University, Bucharest, Romania

Article history
Received: 13-11-2022
Revised: 01-12-2022
Accepted: 06-12-2022

Email: rvvpetrescu@gmail.com

Abstract: The paper presents the study of the dynamics of a general DoF robot, highlighting some important new aspects in the dynamic design of a certain DoF robot. An improved method of positioning the robot in inverse kinematics is presented, then some new aspects in approaching the forces acting on a robot, but also regarding the determination of loads of the rotary actuators. Finally, a study is made of the dynamic functioning of the robot, with new and interesting aspects.

Keywords: Kinematics, Nonlinear Dynamics, Forces, DoF Robot Mechanism, Kinetic Energy Conservation

Introduction

Robots have the role of easing the work of man, taking over all the difficult, tiring, repetitive, dangerous, stressful, and long-lasting tasks in environments hostile to man (polluted, chemical, radioactive, underwater, in space, on mined lands). Thanks to them and the automation made with robots and with robotic cells and automated processing machines, it was possible to move to new industrial eras, in which processing, assembly, and all factory operations are carried out today exclusively with robots, automatically, with high working speeds but also with a high quality of all the final products made, the work of robots in factories and plants being permanent, on three shifts, possibly on Saturdays, without meal breaks, without weekends, without holidays, without pay and unions and demands. The finished products made today by robotics and automation have a superior quality to those previously made with people, they are produced in much larger quantities and faster, without danger to people, machines or products, at low prices and in much more advantageous conditions. The attempts of some very well-trained workers to keep up with the robots have failed and one by one all the jobs that were still performed by humans were replaced by robots.

The so-called danger of leaving us without jobs (which has long been an object of trade union discussions) was resolved naturally, over time, by man moving to other easier, non-dangerous, superior jobs, designing, conceiving, thinking, optimizing, implementing, control, educational, development, activities that can be carried out anywhere, anytime, with the desired breaks, remaining that the material value obtained immediately (now much higher) with robots, is distributed equitably to all working people, robots requiring only certain acquisition costs, implementation, maintenance, plus necessary transport costs. In this way, it was possible to give up the need for human labor and on Sunday (which was sometimes used), a second weekly day off, Saturday and a short day on Friday could be introduced and, in the future, it will be switched to the working week of only four days for man. The man was freed from hard and dangerous work for his health, now having the prospect of working in pleasant environments, only 4-5 days a week, with higher incomes and a much higher standard of living and safety.

In the military field, robots, drones, and other automated components have been helping absolutely all types of military actions for a very long time, today no kind of military operation is possible without the support of robots, drones, automation, and artificial intelligence.

Robots, drones, and artificial intelligence have penetrated almost all fields today, supported by wireless networks (increasingly developed), digitization, computerization, and automation, all evolving rapidly and permanently both by themselves and by the evolution of increasingly modern electronic components (microchips and recently from February 2022 nanochips) but also of increasingly adapted materials (nanomaterials).

It should be emphasized that the essential role of robots is completely different, this being a historical role (today in full swing), namely "the conquest of cosmic space by humanity and the extension of the human species in the universe".

In computer science, Artificial Intelligence (AI) is the intelligence exhibited by machines, as opposed to the natural intelligence exhibited by humans and some animals. Today all machines have advanced artificial intelligence and both the software and the components of artificial thinking evolve very quickly. Modern machine capabilities broadly classified as AI include understanding human speech, competing at the highest level of strategy game systems, autonomous vehicles, and

intelligent routing in content distribution networks, as well as military simulations.

The development of Metal-Oxide-Semiconductor (MOS) Very-Large-Scale Integration (VLSI), in the form of Complementary MOS (CMOS) technology, has allowed the number of MOS transistors to increase in digital electronics.

Automation has come a long way today, with the key role being played by DoF robots of various shapes and sizes.

A 'Degree of Freedom' (DoF) as it relates to robotic arms, is an independent joint that can provide freedom of movement for the manipulator, either in a rotational or translational (linear) sense. Every geometric axis that a joint can rotate around or extend along is counted as a Single Degree of Freedom.

In theory, quite a few types of joints provide varying degrees of freedom in terms of rotation and translation. In practice, however, most robotic arms will be made up of joints that provide one degree of freedom. The two most common joints are:

- Revolute Joint: Providing one degree of rotational freedom
- Prismatic Joint: Providing one degree of linear freedom

As such, robotic arms are often described in terms of how many total DoF they have (Arsenault and Gosselin, 2006; Bandyopadhyay and Ghosal, 2003; Pennestri *et al*., 2005).

Sometimes a 'Degree of freedom' is coopted to be used for a function that does not result in 'freedom'. In other words, it does not move the position or orientation of the end-effector/gripper/tool/sensor (the part of the robot that 'does stuff). For Reach Robotics manipulators, we usually have a set of jaws at the end of the robotic arm. To open or close the jaws of the robotic arm, we use a prismatic actuator (a fancy word for an actuator that only operates along a single axis).

We define the reference point as a floating location between the manipulator's jaws. As the manipulator moves, this location is updated in terms of the 'position' of the end-effector. If you want to grab something at position (x, y, z) with orientation (a, b, c), this position is optimized in the inverse kinematics algorithm.

Because of this, the movement of the linear actuator to open and close the manipulator's gripper does not change the reference point and thus, it is not providing a 'degree-of-freedom.

In this scenario, the prismatic actuator provides a 'function' but not a 'degree of freedom. As such, we may define a manipulator as having a different number of DoF and Functions; for example, the Bravo 7 is a 7-Function, 6 DoF manipulator, with one function being the open/close of the jaws (Fig. 1).

Fig. 1: A DoF4 and a DoF 6 robot. Source: https://reachrobotics.com/media/Article-Imagery-Infographic-01-2-1536x864.jpg

Why is all this important? One of the main things people are interested in when solving a complex robotic manipulator problem is the DoF and its Functions. These two distinct pieces of terminology help to shortcut conversations and make sure everyone is talking on the same page!

It is no longer necessary to talk about the importance of industrial robots, considering that they have recently reached the figure of three million industrial robots installed all over the planet, even if almost two-thirds of them work only in Asia. The benefits brought by them are already known, the fact that they have taken over the heavy, tiring, repetitive jobs in dangerous environments and that they can work non-stop, with high speeds and with very good quality, with very low costs.

Today, however, dynamics cover a multitude of aspects, starting from forces in systems and going to new technologies and technological processes. A methodology for the flexible implementation of collaborative robots in intelligent manufacturing systems is presented in the paper (Giberti *et al*., 2022). A robot arm design optimization method using a kinematic redundancy resolution technique is presented in (Maaroof *et al*., 2021). Trajectory control of industrial robots using multilayer neural networks driven by iterative learning control can be found in the paper (Chen and Wen, 2021).

Dynamic and friction parameters of an industrial robot with repeatability identification, comparison, and analysis are other important aspects of dynamic and robotic processes in the industry (Hao *et al*., 2021). The impact of gravity compensation on reinforcement learning in goal-setting tasks for robotic manipulators is a relatively new problem in dynamic disciplines (Fugal *et al*., 2021). Another dynamic new aspect is the mechatronic redesign of a manual assembly workstation in collaboration with wiring assemblies (Palomba *et al*., 2021), which can be directly associated with new technological processes.

Another aspect of the dynamic process appears in (Yamakawa *et al*., 2021) through the development of a

high-speed, low-latency, remote-controlled robotic manual system. Accessible educational resources for teaching and learning robotics (Pozzi *et al*., 2021) is also a dynamic aspect, but different from the physical-mechanical one that is of particular interest to us in this study. Dynamic identification of the parameters of a pointing mechanism taking into account joint play (Sun *et al*., 2021) is a basic dynamic process. The impact of cycle time and payload of an industrial robot on resource efficiency (Stuhlenmiller *et al*., 2021) is also an important aspect of dynamic processes. Today, adaptive position (or force) control of a robot manipulator (Gierlak, 2021; Geng *et al*., 2021), as well as trajectory control (Colan *et al*., 2021; Liu *et al*., 2021; Engelbrecht *et al*., 2021; Alizade *et al*., 2021; Scalera *et al*., 2021), are important dynamic processes.

Another important dynamic aspect (Essomba, 2021; Miguel-Tomé, 2021) is the balancing of technological processes (Caruso *et al*., 2021; Ebel *et al*., 2021; Thompson *et al*., 2021; Al Younes and Barczyk, 2021; Pacheco-Gutierrez *et al*., 2021; Stodola *et al*., 2021; Raviola *et al*., 2021; Medina and Hacohen, 2021; Malik *et al*., 2021).

The current work starts from the basic structure of the DoF robots, consisting of two mobile elements linked together by a kinematic rotation coupler, each of the two mobile elements (denoted in the work with 1 and 2 respectively, or the left and right element) being actuated by a rotary actuator (Fig. 2).

Rotary motors actuate the mobile elements 1 and 2, in A and B. AB = l1, BC = l2 is the length of the mobile elements 1 and 2, and j_1 (or f_1) and j_2, (or f_2), are the angles that position the mobile elements in relation to the Ox axis. The mass of mobile element 1 is considered concentrated in the center of symmetry S1, while the mass of mobile element 2 will be concentrated in the center of symmetry S2 (Petrescu and Petrescu, 2016; 2021; Petrescu, 2012, 2022).

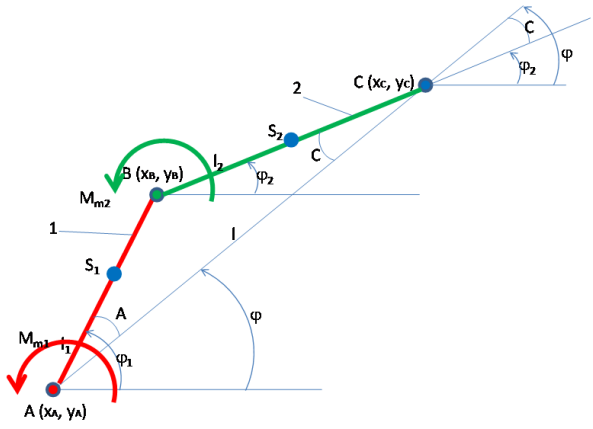

Fig. 2: A basic DoF robot

Methods

The determination of the scalar coordinates of the inner coupling (B) from the 3R mechatronic module can be done (within the Mathcad program used) directly with the "given" function that solves very difficult nonlinear constraints, but it is more elegant to solve this nonlinear mathematical system directly, with an original geometric method (Petrescu, 2012), Eq. (1) and Fig. 3. One knows the constant lengths ls (the length of the element on the left) and ld (the length of the element on the right), of the two movable elements 1 (from the left) and 2 (from the right), respectively, and the scalar coordinates of the ends of the two segments (that is, the coordinates of the points S and D) and the geometric problem is to find the precise scalar coordinates of point C in Fig. 3, a point that connects the two segments 1 and 2, but which can only be in one of the two positions indicated in Fig. 3, that of the top (C'), or bottom (C):

$$\begin{cases} l = SD = \sqrt{(x_D - x_S)^2 + (y_D - y_S)^2}; l_S = SC; l_D = CD; \\ y = y_C = \dfrac{y_D \cdot \left(l^2 + l_S^2 - l_D^2\right) \mp x_D \cdot \sqrt{4l^2 \cdot l_S^2 - \left(l^2 + l_S^2 - l_D^2\right)^2}}{2l^2} + y_S \\ x = x_C = \dfrac{l^2 + l_S^2 - l_D^2 - 2y_D \cdot y_C}{2x_D} + x_S \end{cases} \quad (1)$$

For the DoF mechanism proposed in Fig. 2, Eq. (1) is applied and written in the form (2):

$$\begin{cases} l = AC = \sqrt{(x_C - x_A)^2 + (y_C - y_A)^2}; l_S = AB; l_D = BC; \\ y = y_B = y_A + \dfrac{y_C \cdot \left(l^2 + l_S^2 - l_D^2\right) \mp x_C \cdot \sqrt{4l^2 \cdot l_S^2 - \left(l^2 + l_S^2 - l_D^2\right)^2}}{2l^2} \\ x = x_B = \begin{cases} x_A + \dfrac{l^2 + l_S^2 - l_D^2 - 2y_C \cdot y_B}{2x_C}; pentru\, x_C \neq 0 \\ x_A + \sqrt{l_S^2 - (y_B - y_A)^2}; pentru\, x_C = 0 \end{cases} \end{cases} \quad (2)$$

The original method (Petrescu, 2012) is improved here by eliminating the danger of interruptions that may occur within the equation that generates x_B, and depending on x_C when x_C would take the zero value and a point of discontinuity of the relationships would appear mathematically, the non-linear function continues then becoming a discrete one due to the value x_C positioned at the denominator when it will eventually take the value 0 and it is proposed to replace the direct general expression of x_B (top form) with the expression from the bottom form (which even if it does not have a unique direct solution, it can be used to determine the scalar parameter x_B only at the point where x_C would possibly take the zero value). The method with two expressions for the same value is applied in the calculation program presented in the appendix, by using the logical "if" function.

The trigonometric functions cos (denoted by c) and sin (denoted by s) of the two positioning angles FI1 and FI2 are

now determined, with the help of which the two positioning angles FI1 and FI2 can be precisely calculated (Eq. 3):

$$\begin{cases} c1=\dfrac{x_B-x_A}{l_1};s1=\dfrac{y_B-y_A}{l_1};\varphi_1=sign(s1)\cdot\arccos(c1) \\ c2=\dfrac{x_C-x_B}{l_2};s2=\dfrac{y_C-y_B}{l_2};\varphi_2=sign(s2)\cdot\arccos(c2) \end{cases} \quad (3)$$

Now the scalar parameters (Eq. 4) of the two centers of symmetry S_1 and S_2 can also be determined:

$$\begin{cases} \begin{cases} x_{S_1}=x_A+ls_1\cdot\cos\varphi_1 \\ y_{S_1}=y_A+ls_1\cdot\sin\varphi_1 \end{cases} \\ \begin{cases} x_{S_2}=x_B+ls_2\cdot\cos\varphi_2 \\ y_{S_2}=y_B+ls_2\cdot\sin\varphi_2 \end{cases} \end{cases} \quad (4)$$

Next, is the selection and automation of the motor speeds, when we want constant speeds for the two elements 1 and 2 (Eq. 5; obviously, the sign of the velocities is given by that of the positions-see the appendix):

$$\begin{cases} \omega_1=w_1\cdot sign(\Delta\varphi_1) \\ \omega_2=w_2\cdot sign(\Delta\varphi_2) \end{cases} \quad (5)$$

The angular accelerations are zero except at discrete points where the angular velocities change sign (so they cancel). We can now determine the velocities and accelerations from the couplings B and C and the centers of symmetry S_1 and S_2 (Eq. 6):

$$\begin{cases} \begin{cases} \dot{x}_B=\dot{x}_A-l_1\cdot\sin\varphi_1\cdot\omega_1 \\ \dot{y}_B=\dot{y}_A+l_1\cdot\cos\varphi_1\cdot\omega_1 \end{cases} \begin{cases} \ddot{x}_B=\ddot{x}_A-l_1\cdot\cos\varphi_1\cdot\omega_1^2-l_1\cdot\sin\varphi_1\cdot\varepsilon_1 \\ \ddot{y}_B=\ddot{y}_A+l_1\cdot\sin\varphi_1\cdot\omega_1^2+l_1\cdot\cos\varphi_1\cdot\varepsilon_1 \end{cases} \\ \begin{cases} \dot{x}_{S_1}=\dot{x}_A-ls_1\cdot\sin\varphi_1\cdot\omega_1 \\ \dot{y}_{S_1}=\dot{y}_A+ls_1\cdot\cos\varphi_1\cdot\omega_1 \end{cases} \begin{cases} \ddot{x}_{S_1}=\ddot{x}_A-ls_1\cdot\cos\varphi_1\cdot\omega_1^2-ls_1\cdot\sin\varphi_1\cdot\varepsilon_1 \\ \ddot{y}_{S_1}=\ddot{y}_A-ls_1\cdot\sin\varphi_1\cdot\omega_1^2+ls_1\cdot\cos\varphi_1\cdot\varepsilon_1 \end{cases} \\ \begin{cases} \dot{x}_C=\dot{x}_B-l_2\cdot\sin\varphi_2\cdot\omega_2 \\ \dot{y}_C=\dot{y}_B+l_2\cdot\cos\varphi_2\cdot\omega_2 \end{cases} \begin{cases} \ddot{x}_C=\ddot{x}_B-l_2\cdot\cos\varphi_2\cdot\omega_2^2-l_2\cdot\sin\varphi_2\cdot\varepsilon_2 \\ \ddot{y}_C=\ddot{y}_B-l_2\cdot\sin\varphi_2\cdot\omega_2^2+l_2\cdot\cos\varphi_2\cdot\varepsilon_2 \end{cases} \\ \begin{cases} \dot{x}_{S_2}=\dot{x}_B-ls_2\cdot\sin\varphi_2\cdot\omega_2 \\ \dot{y}_{S_2}=\dot{y}_B+ls_2\cdot\cos\varphi_2\cdot\omega_2 \end{cases} \begin{cases} \ddot{x}_{S_2}=\ddot{x}_B-ls_2\cdot\cos\varphi_2\cdot\omega_2^2-ls_2\cdot\sin\varphi_2\cdot\varepsilon_2 \\ \ddot{y}_{S_2}=\ddot{y}_B-ls_2\cdot\sin\varphi_2\cdot\omega_2^2+ls_2\cdot\cos\varphi_2\cdot\varepsilon_2 \end{cases} \end{cases} \quad (6)$$

Robot Forces

Next is the kinetostatic study of the robot, i.e., the determination of the forces in the mechanism.

Specify the linear and rotational masses of the two mobile elements, the technological resistance R_T acting on point C (end effector), but also specify the mass in C temporarily produced by the force R_T as long as the force R_T exerts an action on point C, where m_C=|RT|/g.

The torsion of the inertial forces acting on the robot is immediately calculated (Eq. 7), where the scalar inertia forces on the x or y axes concentrated in the centers of symmetry of the two elements are calculated as the product of the respective mass and the corresponding scalar acceleration amplified with a minus sign that is introduced to the scalar magnitudes of the force vectors due to the permanent opposition between an inertial force and the acceleration that produces it; also here an innovation of this study is introduced, namely, the introduction of an additional mass by a force of gravity R_T that presses on the robot at point C, the mass being equal to the force of gravity divided by the gravitational acceleration g (for this reason the mass that appears additionally on element 2 at point C, m_C, will produce inertial forces on the two scalar axes of the reference plane, in the point C; see the Fig. 4 and the appendix):

$$\begin{cases} \begin{cases} F_{S_1}^{ix}=-m_1\cdot\ddot{x}_{S_1} \\ F_{S_1}^{iy}=-m_1\cdot(\ddot{y}_{S_1}+g) \\ M_1^i=-J_{S_1}\cdot\varepsilon_1 \end{cases} \begin{cases} F_{S_2}^{ix}=-m_2\cdot\ddot{x}_{S_2} \\ F_{S_2}^{iy}=-m_2\cdot(\ddot{y}_{S_2}+g) \\ M_2^i=-J_{S_2}\cdot\varepsilon_2 \end{cases} \begin{cases} F_C^{ix}=-m_C\cdot\ddot{x}_C \\ F_C^{iy}=-m_C\cdot(\ddot{y}_C+g) \end{cases} \end{cases} \quad (7)$$

In blue are represented the known forces (already calculated with relations 7) and in red are the unknown forces (reactions from couples A and B and also the moments of engines 1 and 2 present at the same points).

The moments and forces acting on the robot are now determined. Initially, a sum of moments relative to point B on mobile element 2 is written, which is equal to zero and from which the moment M_2 is directly determined (Eq. 8).

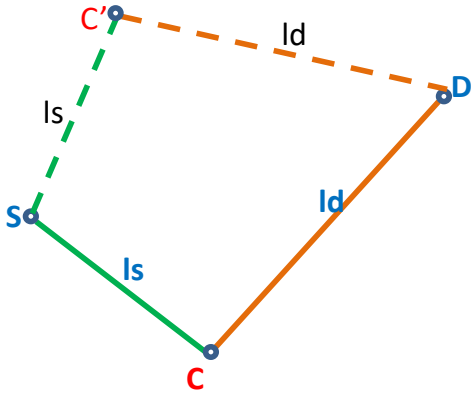

Fig. 3: The positions where the inner point C can be found, up or down

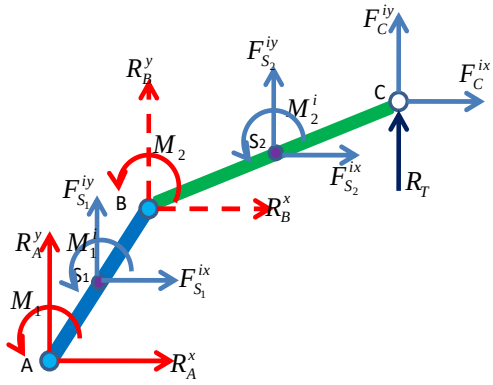

Fig. 4: Forces of the DoF robot

$$\begin{cases}\sum M_B^{(2)}=0\Rightarrow M_2+M_2^i-F_{S_2}^{ix}\cdot\left(y_{S_2}-y_B\right)+\\ F_{S_2}^{iy}\cdot\left(x_{S_2}-x_B\right)-F_C^{ix}\cdot\left(y_C-y_B\right)+F_C^{iy}\cdot\left(x_C-x_B\right)=0\\ M_2=-M_2^i+F_{S_2}^{ix}\cdot\left(y_{S_2}-y_B\right)+F_{S_2}^{iy}\cdot\left(x_B-x_{S_2}\right)+\\ F_C^{ix}\cdot\left(y_C-y_B\right)+F_C^{iy}\cdot\left(x_B-x_C\right)\end{cases} \tag{8}$$

Similarly, a sum of moments relative to point A on elements 2 plus 3 is written, which must be zero, from which the moment M_1 is directly determined (Eq. 9):

$$\begin{cases}\sum M_A^{(1,2)}=0\Rightarrow M_1+M_1^i+M_2+M_2^i-F_{S_1}^{ix}\cdot\left(y_{S_1}-y_A\right)+\\ F_{S_1}^{iy}\cdot\left(x_{S_1}-x_A\right)-F_{S_2}^{ix}\cdot\left(y_{S_2}-y_A\right)+F_{S_2}^{iy}\cdot\left(x_{S_2}-x_A\right)\\ -F_C^{ix}\cdot\left(y_C-y_A\right)+F_C^{iy}\cdot\left(x_C-x_A\right)=0\Rightarrow\\ M_1=-M_1^i-M_2-M_2^i+F_{S_1}^{ix}\cdot\left(y_{S_1}-y_A\right)+\\ F_{S_1}^{iy}\cdot\left(x_A-x_{S_1}\right)+F_{S_2}^{ix}\cdot\left(y_{S_2}-y_A\right)+\\ F_{S_2}^{iy}\cdot\left(x_A-x_{S_2}\right)+F_C^{ix}\cdot\left(y_C-y_A\right)+F_C^{iy}\cdot\left(x_A-x_C\right)\end{cases} \tag{9}$$

The reactions from couples B and A can now be determined through two force balances, on the *x* and *y* scalar axes, respectively, on element 2 and then on mobile element 1 (Eq. 10):

$$\begin{cases}\sum F_x^{(2)}=0\Rightarrow R_B^x+F_{S_2}^{ix}+F_C^{ix}=0\Rightarrow R_B^x=-F_{S_2}^{ix}-F_C^{ix}\\ \sum F_y^{(2)}=0\Rightarrow R_B^y+F_{S_2}^{iy}+F_C^{iy}=0\Rightarrow R_B^y=-F_{S_2}^{iy}-F_C^{iy}\\ \sum F_x^{(1)}=0\Rightarrow R_A^x+F_{S_1}^{ix}+(-R_B^x)=0\Rightarrow R_A^x=R_B^x-F_{S_1}^{ix}\\ \sum F_y^{(1)}=0\Rightarrow R_A^y+F_{S_1}^{iy}+(-R_B^y)=0\Rightarrow R_A^y=R_B^y-F_{S_1}^{iy}\end{cases} \tag{10}$$

Robot Dynamics

The double kinetic energy of the robot is written by summing the components on the two mobile elements 1 and 2, after which the mass moment of inertia of the entire robot mechanism is expressed, reduced either to element 1 or to element 2 (Eq. 11), where DE_c is twice the kinetic energy of the entire robot mechanism; E_c is the kinetic energy of the DoF robot; J_{S1} is the rotational mass of the mobile element 1 and J_{S2} the rotational mass of the element 2; w_1 and w_2 are the rotational (angular) velocities of the mobile elements 1 and 2; ls_1 is the length between points A and S_1 and ls_2 the length between points B and S_2; J^*_{1S1} is the rotational mass of the DoF robot reduced to the element 1 in point S_1 and J^*_{1A} is the rotational mass of the DoF robot reduced to the element 1 in point A; J^*_{2S2} is the rotational mass of the DoF robot reduced to the element 2 in point S_2 and J^*_{2B} is the rotational mass of the DoF robot reduced to the element 2 in point B.

$$\begin{cases}DE_c\equiv 2\cdot E_c=J_{S_1}\cdot\omega_1^2+m_1\cdot\left(\dot{x}_{S_1}^2+\dot{y}_{S_1}^2\right)+\\ J_{S_2}\cdot\omega_2^2+m_2\cdot\left(\dot{x}_{S_2}^2+\dot{y}_{S_2}^2\right)+m_C\cdot\left(\dot{x}_C^2+\dot{y}_C^2\right)\\ J_{1S_1}^*=\dfrac{2\cdot E_c}{\omega_1^2};J_{1A}^*=J_{1S_1}^*+m_1\cdot ls_1^2;\\ J_{2S_2}^*=\dfrac{2\cdot E_c}{\omega_2^2};J_{2B}^*=J_{2S_2}^*+m_2\cdot ls_2^2;\end{cases} \tag{11}$$

One can now simply determine the reduced (i.e., dynamic) angular velocity at moving element 1, or at moving element 2, the resulting angular acceleration by deriving the dynamic angular velocity (Eq. 12), where D_{1i} is the dynamic robot coefficient of the inertia forces on element 1 and D_{2i} is the dynamic coefficient of the inertia forces on element 2; D_c is the dynamic coefficient of the couples (Petrescu, 2012; 2022):

$$\begin{cases}D_c=1;D1_i=\sqrt{\dfrac{J_{1Amed}^*}{J_{1A}^*}};\omega_1^*=D_c\cdot D1_i\cdot\omega_1;\\ \varepsilon_1^*=\omega_1^*\cdot\dfrac{\Delta\omega_1^*}{\Delta\varphi_1}\\ D2_i=\sqrt{\dfrac{J_{2Bmed}^*}{J_{2B}^*}};\omega_2^*=D_c\cdot D2_i\cdot\omega_2;\\ \varepsilon_2^*=\omega_2^*\cdot\dfrac{\Delta\omega_2^*}{\Delta\varphi_2}\end{cases} \tag{12}$$

If we also want to take into account the dynamic effect imposed by the kinematic couplings, the generic value 1 of the dynamic coupling coefficient D_c is replaced by its expression for the related structural module (two kinematic elements linked together by a kinematic rotation coupling C_5, Eq. 13; Petrescu, 2012), see the appendix:

$$D_c=\sin^2(\varphi_1-\varphi_2) \tag{13}$$

Results and Discussion

In the example addressed, the trajectory of the end-effector C was imposed on a circle (Fig. 5) and all the kinematic parameters of the DoF robot operating in inverse kinematics are determined.

The chosen independent constant k takes natural values from 0 to 72, in order not to load the Mathcad system very much. Point B which corresponds to the internal coupling of the robot moves on a trajectory imposed by the one chosen at the end effector C, according to the diagram in Fig. 6.

The angles that position the two mobile elements 1 and 2 vary (in degrees) according to the trajectories indicated in the diagram in Fig. 7.

The angular velocities of the two mobile elements vary according to the diagram in Fig. 8, while the angular velocities of the two actuators have the variation in Fig. 9. Note that motor 1 rotates with angle FI1 with angular speed w1, but motor 2 rotates with FI2-FI1, with angular velocity w2-w1.

The speeds of point B (corresponding to the robot's internal couple) can be seen in the diagram in Fig. 10 and its accelerations in Fig. 11.

The speeds of point C (end effector) can be seen in the diagram in Fig. 12 and its accelerations in Fig. 13.

Next, we follow the same speed and acceleration parameters at points S_1 (Fig. 14-15) and S_2 (Fig. 16-17), respectively, corresponding to the centers of symmetry of the two mobile elements.

The inertial forces of the robot can be seen in the diagram in Fig. 18.

The two motor moments M_1 and M_2, respectively, of the two actuators, can be seen in the diagram in Fig. 19.

The reactions straining motor coupling B are visible in the diagram in Fig. 20 and those stressing motor coupling A can be seen in Fig. 21.

The moments of inertia of the entire robot mechanism reduced to elements 1 or 2, at points S_1 or A, S_2 or B, can be visualized in the diagram in Fig. 22.

The angular velocities of the two mobile elements in both kinematic and dynamic versions can be visualized in the diagram in Fig. 23.

But if we also take into account the influence of the kinematic couplings of the robot (especially the internal coupling B), these values change according to the diagrams in Fig. 24.

A comparison between the kinematic, dynamic, and full dynamic angular velocity (and with the influence of couples), for mobile element 1 of the DoF robot can be seen in Fig. 25 and for element 2 can be seen in Fig. 26.

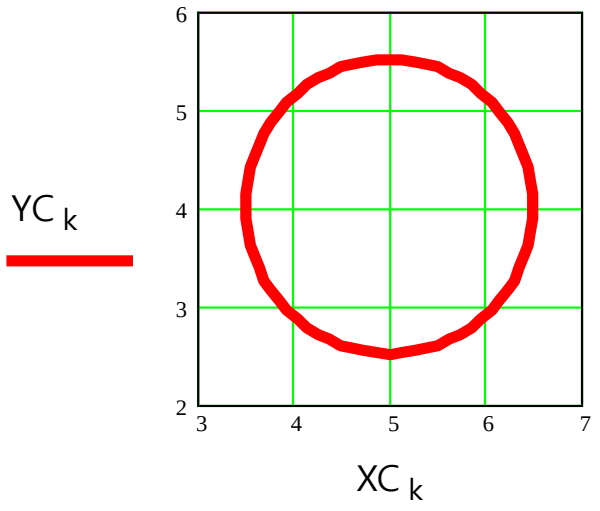

Fig. 5: The trajectory of the end-effector C was imposed on a circle

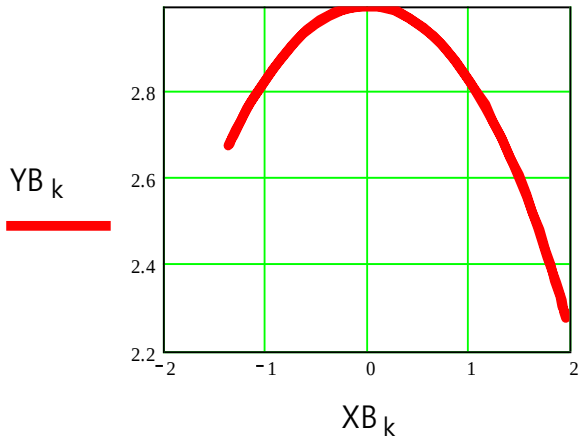

Fig. 6: The trajectory of the point B

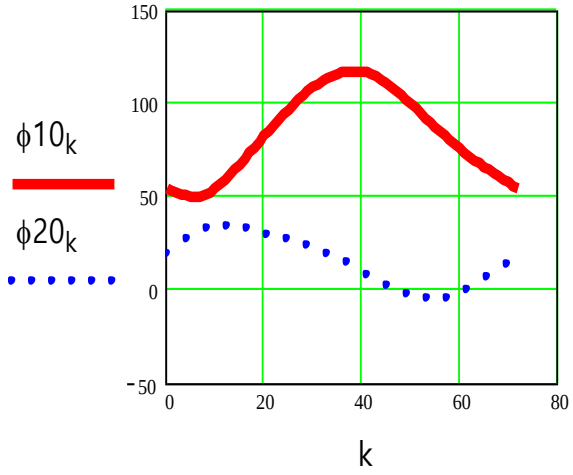

Fig. 7: The angles that position the two mobile elements 1 and 2 (in degrees)

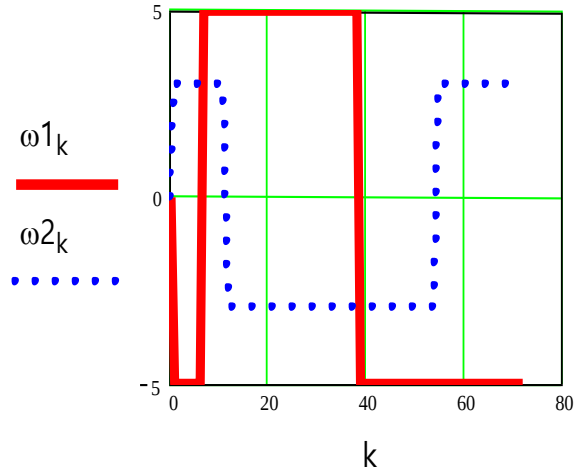

Fig. 8: The angular velocities of the two mobile elements

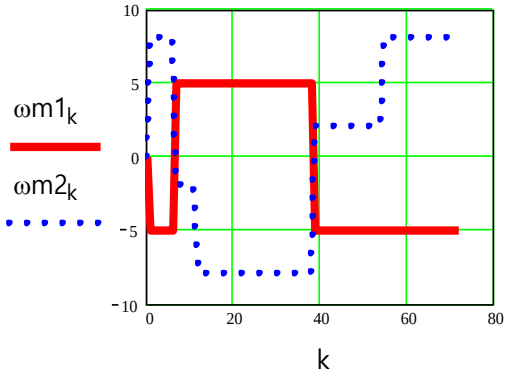

Fig. 9: The angular velocities of the two actuators

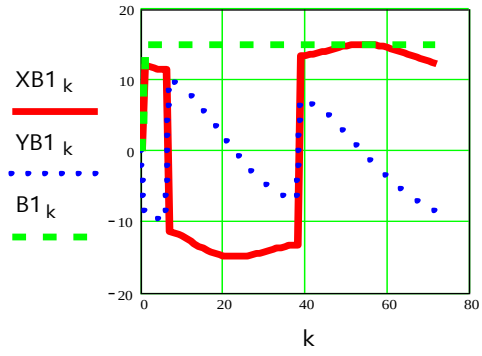

Fig. 10: The speeds of point B

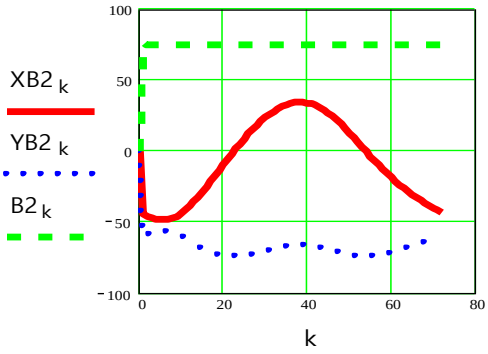

Fig. 11: The accelerations of point B

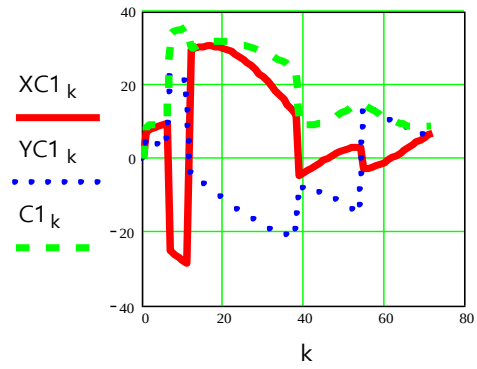

Fig. 12: The speeds of point C

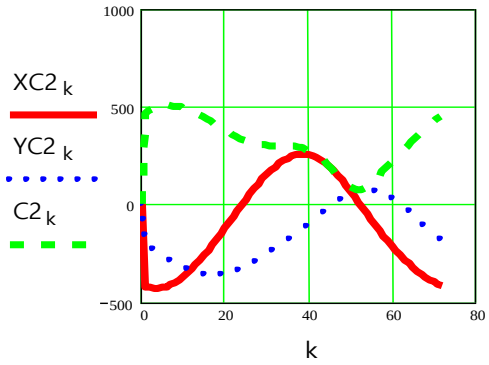

Fig. 13: The accelerations of point C

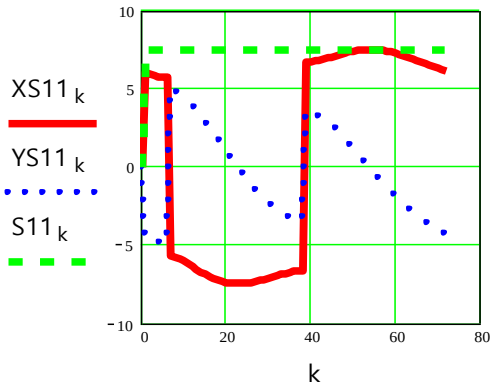

Fig. 14: The speeds of point S_1

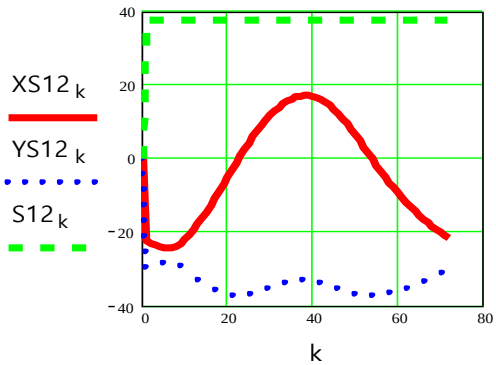

Fig. 15: The accelerations of point S_1

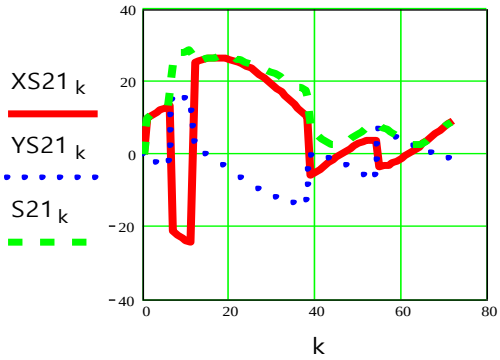

Fig. 16: The speeds of point S_2

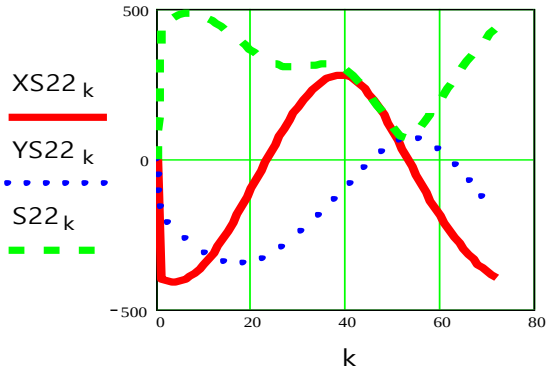

Fig. 17: The accelerations of point S_2

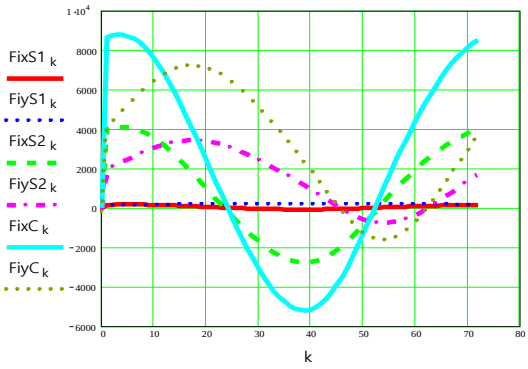

Fig. 18: The inertial forces of the robot

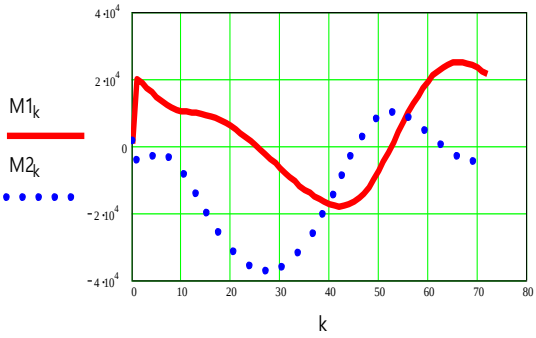

Fig. 19: The two motor moments M_1 and M_2, respectively, of the two actuators

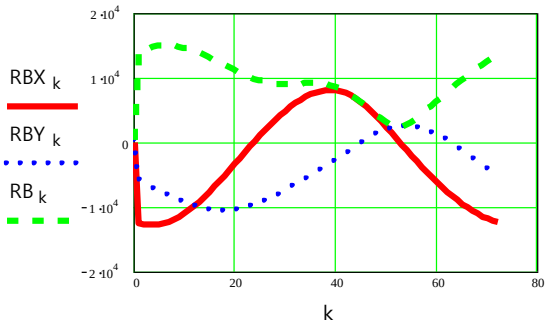

Fig. 20: The reactions straining motor coupling B

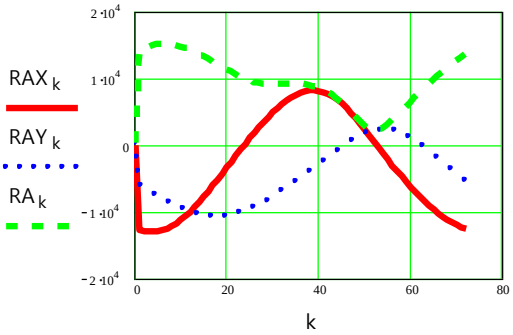

Fig. 21: The reactions stressing motor coupling B

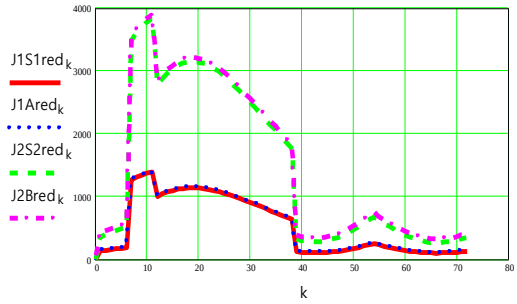

Fig. 22: The moments of inertia of the entire robot mechanism reduced to elements 1 or 2, at points S_1 or A, S_2 or B

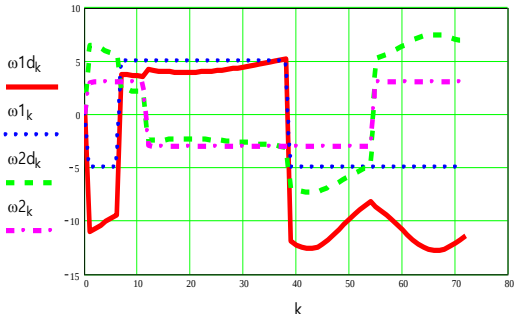

Fig. 23: The angular velocities of the two mobile elements in both kinematic and dynamic versions

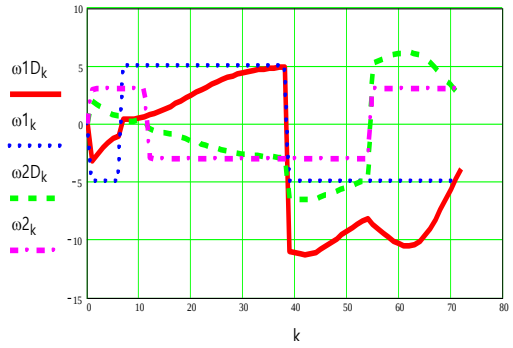

Fig. 24: The angular velocities of the two mobile elements in both kinematic and dynamic versions when one also takes into account the influence of the kinematic couplings of the robot (especially the internal coupling B)

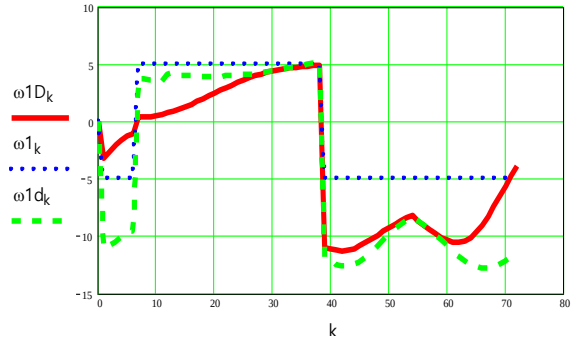

Fig. 25: A comparison between the kinematic, dynamic, and full dynamic angular velocity (and with the influence of couples), for mobile element 1

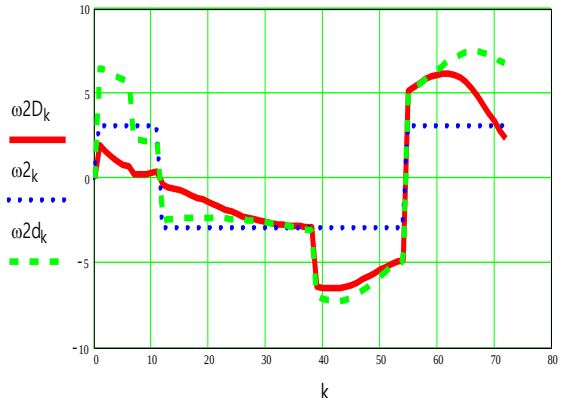

Fig. 26: A comparison between the kinematic, dynamic, and full dynamic angular velocity (and with the influence of couples), for mobile element 2

Conclusion

The paper presents the study of the dynamics of a general DoF robot, highlighting some important new aspects in the dynamic design of a certain DoF robot. An improved method of positioning the robot in inverse kinematics is presented, then some new aspects in approaching the forces acting on a robot, but also regarding the determination of loads of the rotary actuators. Finally, a study is made of the dynamic functioning of the robot, with new and interesting aspects.

The robot mechanism presented in the work is a pivoting column that supports and rotates at 360 degrees a basic DoF planar robot. The method is simple to implement on any type of controller, a PID controller being simply designed and adapted thanks to this new method proposed in the current work, a method that can be generalized.

As you can see, the dynamics of the mechanism determined in two simple steps allows the calculation and plotting of the dynamic parameters very simply, in just two steps, the first being a classic one obtained by conservation of kinetic energy and the second step being a modern one where kinetic energy conservation is also used a second time, thus avoiding the need to use classical laborious methods, such as Newton's differential equations, the Lagrange equation of 1st order (for this mechanism), the Laplace transform or the Fourier integral, or various finite difference methods.

The diagrams simulated in Mathcad are followed, by the kinematics, forces, and dynamic operation of the entire robot DoF or considered on its mobile elements separately. A more precise dynamic study is also presented in which the influence of the kinematic couples that connect the mobile elements is also taken into account.

Acknowledgment

This text was acknowledged and appreciated by Dr. Veturia CHIROIU Honorific member of the Technical Sciences Academy of Romania (ASTR) Ph.D. supervisor in Mechanical Engineering.

Funding Information

Research contract: Contract number 36-5-4D/1986 from 24IV1985, beneficiary CNST RO (Romanian National Center for Science and Technology) Improving dynamic mechanisms internal combustion engines.

Ethics

This article is original and contains unpublished material. The author declares that are no ethical issues and no conflict of interest that may arise after the publication of this manuscript.

References

Al Younes, Y., & Barczyk, M. (2021). Nonlinear model predictive horizon for optimal trajectory generation. *Robotics*, *10*(3), 90. https://doi.org/10.3390/robotics10030090

Arsenault, M., & Gosselin, C. M. (2006). Kinematic, static and dynamic analysis of a spatial three-degree-of-freedom tensegrity mechanism. https://doi.org/10.1115/1.2218881

Bandyopadhyay, S., & Ghosal, A. (2003, January). Analytical Determination of Principal Twists and Singular Directions in Robot Manipulators. In *International Design Engineering Technical Conferences and Computers and Information in Engineering Conference* (Vol. 37009, pp. 1095-1106).https://doi.org/10.1115/DETC2003/DAC-48819

Caruso, M., Gallina, P., & Seriani, S. (2021). On the Modelling of Tethered Mobile Robots as Redundant Manipulators. *Robotics*, *10*(2), 81. https://doi.org/10.3390/robotics10020081

Chen, S., & Wen, J. T. (2021). Industrial robot trajectory tracking control using multi-layer neural networks trained by iterative learning control. *Robotics*, *10*(1), 50. https://doi.org/10.3390/robotics10010050

Colan, J., Nakanishi, J., Aoyama, T., & Hasegawa, Y. (2021). Optimization-based constrained trajectory generation for robot-assisted stitching in endonasal surgery. *Robotics*, *10*(1), 27. https://doi.org/10.3390/robotics10010027

Ebel, L. C., Maaß, J., Zuther, P., & Sheikhi, S. (2021). Trajectory Extrapolation for Manual Robot Remote Welding. *Robotics*, *10*(2), 77. https://doi.org/10.3390/robotics10020077

Engelbrecht, D., Steyn, N., & Djouani, K. (2021). Adaptive Virtual Impedance Control of a Mobile Multi-Robot System. *Robotics*, *10*(1), 19. https://doi.org/10.3390/robotics10010019

Essomba, T. (2021). Design of a five-degrees of freedom statically balanced mechanism with multi-directional functionality. *Robotics*, *10*(1), 11. https://doi.org/10.3390/robotics10010011

Fugal, J., Bae, J., & Poonawala, H. A. (2021). On the impact of gravity compensation on reinforcement learning in goal-reaching tasks for robotic manipulators. *Robotics*, *10*(1), 46. https://doi.org/10.3390/robotics10010046

Geng, J., Arakelian, V., Chablat, D., & Lemoine, P. (2021). Balancing of the Orthoglide taking into account its varying payload. *Robotics*, *10*(1), 30. https://doi.org/10.3390/robotics10010030

Giberti, H., Abbattista, T., Carnevale, M., Giagu, L., & Cristini, F. (2022). A Methodology for Flexible Implementation of Collaborative Robots in Smart Manufacturing Systems. *Robotics*, *11*(1), 9. https://doi.org/10.3390/robotics11010009

Gierlak, P. (2021). Adaptive position/force control of a robotic manipulator in contact with a flexible and uncertain environment. *Robotics*, *10*(1), 32. https://doi.org/10.3390/robotics10010032

Hao, L., Pagani, R., Beschi, M., & Legnani, G. (2021). Dynamic and friction parameters of an industrial robot: Identification, comparison and repetitiveness analysis. *Robotics*, *10*(1), 49. https://doi.org/10.3390/robotics10010049

Liu, R., Nageotte, F., Zanne, P., de Mathelin, M., & Dresp-Langley, B. (2021). Deep reinforcement learning for the control of robotic manipulation: A focussed mini-review. *Robotics*, *10*(1), 22. https://doi.org/10.3390/robotics10010022

Maaroof, O. W., Dede, M. İ. C., & Aydin, L. (2021). A Robot Arm Design Optimization Method by Using a Kinematic Redundancy Resolution Technique. *Robotics*, *11*(1), 1. https://doi.org/10.3390/robotics11010001

Malik, A., Henderson, T., & Prazenica, R. (2021). Multi-Objective Swarm Intelligence Trajectory Generation for a 7 Degree of Freedom Robotic Manipulator. *Robotics*, *10*(4), 127. https://doi.org/10.3390/robotics10040127

Medina, O., & Hacohen, S. (2021). Overcoming Kinematic Singularities for Motion Control in a Caster Wheeled Omnidirectional Robot. *Robotics*, *10*(4), 133. https://doi.org/10.3390/robotics10040133

Miguel-Tomé, S. (2021). The Heuristic of Directional Qualitative Semantic: A New Heuristic for Making Decisions about Spinning with Qualitative Reasoning. *Robotics*, *10*(1), 17. https://doi.org/10.3390/robotics10010017

Pacheco-Gutierrez, S., Niu, H., Caliskanelli, I., & Skilton, R. (2021). A Multiple Level-of-Detail 3D Data Transmission Approach for Low-Latency Remote Visualisation in Teleoperation Tasks. *Robotics*, *10*(3), 89. https://doi.org/10.3390/robotics10030089

Palomba, I., Gualtieri, L., Rojas, R., Rauch, E., Vidoni, R., & Ghedin, A. (2021). Mechatronic re-design of a manual assembly workstation into a collaborative one for wire harness assemblies. *Robotics*, *10*(1), 43. https://doi.org/10.3390/robotics10010043

Pennestri, E., Cavacece, M., & Vita, L. (2005, January). On the computation of degrees-of-freedom: A didactic perspective. In *International Design Engineering Technical Conferences and Computers and Information in Engineering Conference* (Vol. 47438, pp. 1733-1741). https://doi.org/10.1115/DETC2005-84109

Petrescu, F. I. T. (2022). Advanced Dynamics Processes Applied to an Articulated Robot. *Processes*, *10*(4), 640. https://doi.org/10.3390/pr10040640

Petrescu, F. I. T. (2012). Theory of Mechanisms: Course and Applications, CreateSpace Independent Publishing Platform (September 12, 2012), Romanian Paperback: p, 286, ISBN-13: 978-1479302338. https://www.amazon.com/gp/product/1479302333

Petrescu, F. I. T., & Petrescu, R. V. V. (2021). Direct kinematics of a manipulator with three mobilities. *Independent Journal of Management & Production*, *12*(7), 1875-1900. https://doi.org/10.14807/ijmp.v12i7.1160

Petrescu, F. I., & Petrescu, R. V. (2016). Dynamic cinematic to a structure 2R. *GEINTEC Journal*, *6*(2). https://papers.ssrn.com/sol3/papers.cfm?abstract_id=3074369

Pozzi, M., Prattichizzo, D., & Malvezzi, M. (2021). Accessible educational resources for teaching and learning robotics. *Robotics*, *10*(1), 38. https://doi.org/10.3390/robotics10010038

Raviola, A., Guida, R., De Martin, A., Pastorelli, S., Mauro, S., & Sorli, M. (2021). Effects of temperature and mounting configuration on the dynamic parameter's identification of industrial robots. *Robotics*, *10*(3), 83. https://doi.org/10.3390/robotics10030083

Scalera, L., Seriani, S., Gallina, P., Lentini, M., & Gasparetto, A. (2021). Human–robot interaction through eye tracking for artistic drawing. *Robotics*, *10*(2), 54. https://doi.org/10.3390/robotics10020054

Stodola, M., Rajchl, M., Brablc, M., Frolík, S., & Křivánek, V. (2021). Maxwell Points of Dynamical Control Systems Based on Vertical Rolling Disc-Numerical Solutions. *Robotics*, *10*(3), 88. https://doi.org/10.3390/robotics10030088

Stuhlenmiller, F., Weyand, S., Jungblut, J., Schebek, L., Clever, D., & Rinderknecht, S. (2021). Impact of Cycle Time and Payload of an Industrial Robot on Resource Efficiency. *Robotics*, *10*(1), 33. https://doi.org/10.3390/robotics10010033

Sun, J., Han, X., Li, T., & Li, S. (2021). Dynamic Parameter Identification of a Pointing Mechanism Considering the Joint Clearance. *Robotics*, *10*(1), 36.https://doi.org/10.3390/robotics10010036

Thompson, L. A., Badache, M., Brusamolin, J. A. R., Savadkoohi, M., Guise, J., Paiva, G. V. D., ... & Shetty, D. (2021). Multidirectional Overground Robotic Training Leads to Improvements in Balance in Older Adults. *Robotics*, *10*(3), 101. https://doi.org/10.3390/robotics10030101

Yamakawa, Y., Katsuki, Y., Watanabe, Y., & Ishikawa, M. (2021). Development of a high-speed, low-latency telemanipulated robot hand system. *Robotics*, *10*(1), 41. https://doi.org/10.3390/robotics10010041

Appendix

Establishing geometro-kinematic parameters and the independent variable k and the entry angle a:

IS := 3
ID := 5
r := 1.5
XD := 5
YD := 4
XA := 0
YA := 0
k := 72

$$\alpha_k := 2\cdot\pi\cdot\frac{k}{72}$$

I1 := IS
I2 := ID

$$Is1 := \frac{I1}{2}$$

$$Is2 := \frac{I2}{2}$$

Establishing the parameters of point C:

$$XC_k := XD + r\cdot\cos\left(\alpha_k\right)$$
$$YC_k := YD + r\cdot\sin\left(\alpha_k\right)$$

Establishing the parameters of point B:

$$I_k := \sqrt{\left(XC_k - XA\right)^2 + \left(YC_k - YA\right)^2}$$
$$YB_k := YA + \frac{YC_k\cdot\left[\left(I_k\right)^2 + IS^2 - ID^2\right] + XC_k\cdot\sqrt{4\cdot\left(I_k\right)^2\cdot IS^2 - \left[\left(I_k\right)^2 IS^2 - ID^2\right]^2}}{2\cdot\left(I_k\right)^2}$$
$$XB_k := XA + if\left[XC_k = 0, \sqrt{IS^2 - \left(YB_k - YA\right)^2}, \frac{\left(I_k\right)^2 + IS^2 - ID^2 - 2\cdot YC_k\cdot YB_k}{2\cdot XC_k}\right]$$

Establishing FI1 and FI2 parameters:

$$c1_k := \frac{\left(XB_k - XA\right)}{I1}$$
$$s1_k := \frac{\left(YB_k - YA\right)}{I1}$$
$$\phi 1_k := sign\left(s1_k\right)\cdot a\cos\left(c1_k\right)$$
$$\phi 10_k := \phi 1_k\cdot\frac{180}{\pi}$$
$$c2_k := \frac{\left(XC_k - XB_k\right)}{I2}$$
$$s2_k := \frac{\left(YC_k - YB_k\right)}{I2}$$
$$\phi s_k := sign\left(s2_k\right)\cdot a\cos\left(c2_k\right)$$
$$\phi 20_k := \phi 2_k\cdot\frac{180}{\pi}$$

Determining the parameters of points S_1 and S_2:

$$XS1_k := XA + Is1\cdot\cos\left(\phi 1_k\right)$$
$$YS1_k := YA + Is1\cdot\sin\left(\phi 1_k\right)$$
$$XS2_k := XB_k + Is2\cdot\cos\left(\phi 2_k\right)$$
$$YS2_k := YB_k + Is2\cdot\sin\left(\phi 2_k\right)$$

Determination of speeds and accelerations:

$$w1 := 5$$
$$\omega 1_k := if\left(k_{<1,0}, w1 \cdot sign\left(\phi 1_k - \phi 1_{k-1}\right)\right)$$
$$w2 := 3$$
$$\omega 2_k := if\left(k_{<1,0}, w2 \cdot sign\left(\phi 2_k - \phi 2_{k-1}\right)\right)$$
$$\omega m1_k := \omega 1_k$$
$$\omega m2_k := \omega 2_k - \omega 1_k$$
$$\varepsilon 1 := 0$$
$$\varepsilon 2 := 0$$

Determining speeds and accelerations of point B:

$$XB1_k := -I1 \cdot \sin\left(\phi 1_k\right) \cdot \omega 1_k$$
$$XB2_k := -I1 \cdot \cos\left(\phi 1_k\right) \cdot \omega 1_k$$
$$B1_k := \sqrt{\left(XB1_k\right)^2 + \left(YB1_k\right)^2}$$
$$YB2_k := -I1 \cdot \sin\left(\phi 1_k\right) \cdot \left(\omega 1_k\right)^2$$
$$B2_k := \sqrt{\left(XB2_k\right)^2 + \left(YB2_k\right)^2}$$

Determining speeds and accelerations of point C:

$$XC2_k := XB2_k - I2 \cdot \cos\left(\phi 2_k\right) \cdot \left(\omega 2_k\right)^2$$
$$XC1_k := XB1_k - I2 \cdot \sin\left(\phi 2_k\right) \cdot \omega 2_k$$
$$YC1_k := YB1_k + I2 \cdot \cos\left(\phi 2_k\right) \cdot \omega 2_k$$
$$C1_k := \sqrt{\left(XC1_k\right)^2 + \left(YC1_k\right)^2}$$
$$YC2_k := YB2_k - I2 \cdot \sin\left(\phi 2_k\right) \cdot \left(\omega 2_k\right)^2$$
$$C2_k := \sqrt{\left(XC2_k\right)^2 + \left(YC2_k\right)^2}$$

Determining speeds and accelerations of point S_1:

$$XS11_k := -Is1 \cdot \sin\left(\phi 1_k\right) \cdot \omega 1_k$$
$$XS12_k := Is1 \cdot \cos\left(\phi 1_k\right) \cdot \left(\omega 1_k\right)^2$$
$$YS11_k := Is1 \cdot \cos\left(\phi 1_k\right) \cdot \omega 1_k$$
$$S11_k := \sqrt{\left(XS11_k\right)^2 + \left(YS11_k\right)^2}$$
$$YS12_k := -Is1 \cdot \sin\left(\phi 1_k\right) \cdot \left(\omega 1_k\right)^2$$
$$S12_k := \sqrt{\left(XS12_k\right)^2 + \left(YS12_k\right)^2}$$

Determining speeds and accelerations of point S_2:

$$XS22_k := XB2_k - Is2 \cdot \cos\left(\phi 2_k\right) \cdot \left(\omega 2_k\right)^2$$
$$XS21_k := XB1_k - Is2 \cdot \sin\left(\phi 2_k\right) \cdot \omega 2_k$$
$$YS21_k := YB1_k + Is2 \cdot \cos\left(\phi 2_k\right) \cdot \omega 2_k$$
$$S21_k := \sqrt{\left(XS21_k\right)^2 + \left(YS21_k\right)^2}$$
$$YS22_k := YB2_k - Is2 \cdot \sin\left(\phi 2_k\right) \cdot \left(\omega 2_k\right)^2$$
$$S22_k := \sqrt{\left(XS22_k\right)^2 + \left(YS22_k\right)^2}$$

DYNAMICS-Kinetostatics:

$$m1 :=_2 \cdot I1$$
$$m2 :=_2 \cdot I2$$
$$JS1 := m1 \cdot \frac{I1^2}{12}$$
$$JS2 := m2 \cdot \frac{I2^2}{12}$$
$$RT := -200$$
$$g := 9.81$$
$$mC := \frac{|RT|}{g}$$
$$FixS1_k := -m1 \cdot XS12_k$$
$$FiyS1_k := -m1 \cdot \left(YS12_k + g\right)$$
$$Mi1 := -JS1 \cdot \varepsilon 1$$
$$FixS2_k := -m2 \cdot XS22_k$$
$$FiyS2_k := -m2 \cdot \left(XS22_k + g\right)$$
$$Mi2 := -JS2 \cdot \varepsilon 2$$
$$FixC_k := -mC \cdot CX2_k$$
$$FiyC_k := -mC \cdot \left(YC2_k + g\right)$$
$$M2_k := FixS2_k \cdot \left(YS2_k - YB_k\right) + FiyS2_k \cdot \left(XB_k - XS2_k\right)$$
$$+FixC_k \cdot \left(YC_k - YB_k\right) + FiyC_k \cdot \left(XB_k - XC_k\right) - Mi2$$
$$M1_k := FixS1_k \cdot \left(YS1_k - YA\right) + FiyS1_k \cdot \left(XA - XS1_k\right)$$
$$+FixS2_k \cdot \left(YS2_k - YA\right) + FiyS2_k \cdot \left(XA - XS2_k\right) + FixC_k$$
$$\left(YC_k - YA\right) + FiyC_k \cdot \left(XA - XC_k\right) - Mi1 - Mi2 - M2_k$$
$$RBX_k := -FixS2_k - FixC_k$$
$$RBY_k := -FiyS2_k - FiyC_k$$
$$RB_k := \sqrt{\left(RBX_k\right)^2 + \left(RBY_k\right)^2}$$
$$RAX_k := RBX_k - FixS1_k$$
$$RAY_k := RBY_k - FiyS1_k$$
$$RA_k := \sqrt{\left(RAX_k\right)^2 + \left(RAY_k\right)^2}$$

Dynamics-Dynamic operation:

$$DEc_k := JS1 \cdot \left(\omega 1_k\right)^2 + m1 \cdot \left[\left(XS11_k\right)^2 + \left(YS11_k\right)^2\right] + JS2$$

$$\cdot \left(\omega 2_k\right)^2 + m2 \cdot \left[\left(XS21_k\right)^2 + \left(YS21_k\right)^2\right] + mC \cdot \left[\left(XC1_k\right)^2 + \left(YC1_k\right)^2\right]$$

$$J1S1red_k := \frac{DEc_k}{\left(\omega 1_k\right)^2}$$

$$J2S2red_k := \frac{DEc_k}{\left(\omega 2_k\right)^2}$$

$$J1Ared_k := J1S1red_k + m1 \cdot Is1^2$$

$$J2Bred_k := J2S2red_k + m2 \cdot Is2^2$$

$$D2i_k := \sqrt{\frac{\left(\max\left(J2Bred\right) + \min\left(J2Bred\right)\right)}{2 \cdot J2Bred_k}}$$

$$Dc_k := 1$$

$$D1i_k := \sqrt{\frac{\left(\max\left(J1Ared\right) + \min\left(J1Ared\right)\right)}{2 \cdot J1Ared_k}}$$

$$\omega 1d_k := D1i_k \cdot Dc_k \cdot \omega 1_k$$

$$\varepsilon 1d_k := \omega 1d_k \cdot if\left[k_{<1,0}, \frac{\left(\omega 1d_k - \omega 1d_{k-1}\right)}{\phi 1_k - \phi 1_{k-1}}\right]$$

$$\omega 2d_k := D2i_k \cdot Dc_k \cdot \omega 2_k$$

$$\varepsilon 2d_k := \omega 2d_k \cdot if\left[k_{<1,0}, \frac{\left(\omega 2d_k - \omega 2d_{k-1}\right)}{\phi 1_k - \phi 1_{k-1}}\right]$$

$$Dc_k := \left(\sin\left(\phi 1_k - \phi 2_k\right)\right)^2$$

$$\omega 1D_k := D1i_k \cdot Dc_k \cdot \omega 1_k$$

$$\varepsilon 1D_k := \omega 1d_k \cdot if\left[k_{<1,0}, \frac{\left(\omega 1d_k - \omega 1d_{k-1}\right)}{\phi 1_k - \phi 1_{k-1}}\right]$$

$$\omega 2D_k := D2i_k \cdot Dc_k \cdot \omega 2_k$$

$$\varepsilon 2D_k := \omega 2d_k \cdot if\left[k_{<1,0}, \frac{\left(\omega 2d_k - \omega 2d_{k-1}\right)}{\phi 1_k - \phi 1_{k-1}}\right]$$